Non-assisted flare performance at low-flow (<100 MSCFD) conditions

Jenna E. Stolzman[1], Ashray Mohit[1], Luis Gutierrez[2], Jesse Capecelatro[1,3] and Margaret S. Wooldridge[1,3]

[1]Department of Mechanical Engineering, University of Michigan, Ann Arbor, USA

[2]Fluid Engineering Department, Southwest Research Institute, San Antonio, USA

[3]Department of Aerospace Engineering, University of Michigan, Ann Arbor, USA

Abstract

Flaring serves as an important safety tool in various industrial settings such as refineries, chemical processes, natural-gas processing, landfills and more. Low-flow (less than 100 thousand cubic feet per day, MSCFD) flares constitute over 89% of flares in the Permian, Eagle Ford, and Bakken regions of the United States. However, there is limited data on flare performance at these low-flow conditions, particularly with high heating value gases, compositions that may be expected from storage vent tanks and other sources. Flares connected to storage vent tanks may lack access to power, making non-assisted flares (as opposed to steam- or air assisted flares) the preferred choice for remote operation of low-flow waste gases, yet there are few available data on the performance of non-assisted flares at industry relevant conditions. As a result, low-flow, non-assisted flares are the primary focus of this work.

The current study examined the impact of heating value, flow rate, and crosswind conditions on important flare metrics such as combustion efficiency and methane destruction efficiency. A new outdoor experimental facility was created for the study where crosswind velocity was controlled using a blower oriented orthogonal to the axis of the flare flow. The flare plume was captured using an adjustable hood that tracked the plume orientation during different levels of crosswind. Emissions from the flare were determined by sampling the gas from the exhaust hood and using a suite of diagnostics to quantify CO_2, CO, CH_4 and trace hydrocarbons. The combustion and methane destruction efficiencies were determined for the test matrix of conditions. Flare gas compositions included natural gas and a mixture of propane and natural gas, with heating values typical of vent gases from storage tanks. The findings from the study provide insight into the parameters affecting non-assisted flare performance under challenging conditions, such as low-flow gases with high crosswind velocities. This research contributes to the broader objective of improving flare performance in real-world applications.

Keywords: non-assisted flare, methane emissions, storage tank vent gases, low-flow flare, oil and gas, combustion efficiency, destruction efficiency, flare performance

I. Introduction

Flares are used throughout the oil and gas supply chain from upstream extraction and production, through midstream distribution and storage, to downstream refining operations. A flare is a safety device used to relieve pressure from operations by burning excess or waste gas in lieu of venting harmful toxins to the environment. Within the oil and gas industry, flares serve multiple purposes: temporary flaring during well completions, flaring during maintenance activities or startup and shutdowns, in response to system upsets, etc. [1]. It is assumed that flares meeting United States (US) Code of Federal Regulations (CFR) design specifications, such as minimum heating value and maximum tip velocity, destroy 98% of hydrocarbons entering the flare tip [2]. However, a recent airborne study by Plant et al. [3] found that flaring releases up to five times more methane to the atmosphere compared with EPA estimates, decreasing the effective methane destruction removal efficiency to as low as 91.1%.

Flare designs vary broadly based on expected operating parameters, the needs of the site, and regulation requirements. They may include an assist-medium, such as air or steam, to enhance combustion and reduce visible smoke emissions [1,4]. Steam-assisted flares are commonly used in refining applications where soot mitigation is required, and a boiler is available on site to generate steam. Air-assisted flares are an alternative for refineries lacking steam or at production sites with available power [4]. Non-assisted flares

(i.e., without any assist-medium) are used more frequently at production sites where soot may not be a concern, particularly in remote locations without access to power. There have been several large-scale flare studies conducted throughout the 1980s and 2010s [5,6,7,8,9,10,11] with the primary findings including that the heating value and exit velocity of the waste gas and amount of assist medium used significantly impact flare performance. While these studies are extremely insightful, most of these studies focused on flare designs and operating conditions typical of refinery or downstream flares, and the studies primarily used steam- and air-assisted flares. Sites with limited-to-no access to power, such as production sites and storage tanks, use non-assisted flares. These types of flares differ significantly from refinery flare conditions and few studies exist of non-assisted flares. The associated flow rates are typically low, less than 50 thousand cubic feet per day (MSCFD) and heating values can range from 1,000 to 2,500 BTU/scf. Furthermore, 2018 estimates show that of the 78,000 flares in operation in the Bakken, Eagle Ford, and Permian basins in the US, 89% operate at flow rates at or below 100 MSCFD [12]. These low-flow flares comprise over 26% of the total flare volume in these regions, making low-flow, non-assisted flares an important market segment and the target for this study.

While fewer studies have been conducted on non-assisted flares, there are some important results in the literature. Pohl et al. [7] conducted outdoor tests on 3", 6", and 12" flare tips using propane diluted with varying amounts of nitrogen as the fuel source over a range of flare-tip exit velocities. They observed high (>95%) combustion efficiency until the heating value decreased below approximately 500 BTU/scf. While the higher heating value fuels had higher combustion efficiency (CE), smoking was observed, which is against US regulations [2]. It should be noted that the study by Pohl et al. was completed in an ambient environment where crosswind was low (less than 8 miles per hour (MPH)). Research on non-assisted flares in wind-tunnel environments has assessed the impact of increased crosswind on performance. Johnson and Kostiuk [13] studied 0.5" – 2" non-assisted pipe flares in a closed-loop wind tunnel, examining the effects of flare gas flow rates, composition, burner diameters, and crosswind speeds on performance. They found smaller pipe diameters, increased crosswind velocities, and low heating value gases negatively impacted performance, while increased flare gas exit velocity made the flames more resistant to crosswind effects. They also found that a turbulent crosswind decreased combustion efficiency compared with a laminar crosswind. Howell [14] expanded their work by evaluating 1" – 4" natural gas pipe flares, reaching similar conclusions and developing similar scaling parameters. Gogolek [15] performed open-loop wind tunnel experiments with pipe flares ranging in diameter from 1" to 6", developing a new scaling parameter and finding that flares with diameters less than 3" did not scale similarly as larger diameter flares. Recently, Burtt [16] investigated 1" – 4" diameter pipe flares in a wind-tunnel with a turbulent crosswind, comparing various scaling laws and developing empirical models for 2" to 4" diameter flares with low (<20% by volume) inert gas in the flare gas. While wind tunnel studies provide invaluable information on flare performance with controlled environmental conditions; field-specific effects, such as dynamic flare operation and environmental transients, may not be captured. Previous work by Stolzman et al. [17,18] tested various non-assisted flare tips, including a 3" pipe, and evaluated effects of heating value, gas flow rate, crosswind, and tip geometry on performance. The experiments were completed in an indoor environment with a calorimeter to capture combustion products and a fan to generate up to 13 miles per hour (MPH) crosswind at the flare tip. Like other studies, they found higher flare-gas flow rates and heating values improved combustion efficiency while low-flow flare-gas conditions with lower heating values were significantly affected by crosswind. Additionally, they found at low gas flow rates, the flare tip geometry impacted performance with a new tip design showing improved performance compared with a baseline utility pipe flare configuration.

The objective of this study aims to expand the previous work by Stolzman et al. [17,18] by: (i) demonstrating a new methodology for evaluating performance of non-assisted flares at flare-gas flow rates up to 50 MSCFD and crosswind speeds up to 40 MPH using an outdoor testing facility and (ii) assessing the performance of a 3" open pipe flare tip over an expanded range of conditions relevant to flares connected to storage vent tanks and other non-assisted flare operation. An adjustable hood was used to collect the flare emissions and extractive sampling techniques were used for measurement of the species in the flare plume. Associated combustion and methane destruction efficiencies were calculated and related uncertainty

analysis was conducted. The results are compared with prior studies and discussed in the context of broader understanding of non-assisted flare behavior.

II. Experimental set up and methodology

i. Experimental set up

A new experimental set-up and protocols were created at an outdoor facility at Southwest Research Institute. The outdoor setup provided a semi-controlled environment for measurement of flare performance. A schematic of the facility is shown in **Fig. 1.** Crosswind conditions were controlled using a blower ('Blower 1' in **Fig. 1**) with a variable frequency driver capable of generating up to 40 miles per hour (MPH) crosswind at the flare tip. The crosswind velocity was measured during the experiments upstream of the flare tip, using a series of hot wire anemometers (Degree Controls F500) with a sampling rate of 1 second.

An exhaust hood for capturing combustion products measured 6x6 feet in cross-section and was mounted to a rig that allowed for translation (i.e., moving it closer and further from the flare tip) and rotation through the use of motors. The exhaust hood was connected to a blower ('Blower 2' in **Fig. 1**) with a variable frequency driver to control the speed of the exhaust flow.

Two methods were used to ensure a significant fraction of the flare plume was captured by the hood and that the combustion reactions were complete: (i) a thermocouple placed inside the hood continuously measured the temperature of the gases to ensure the plume temperature was below 120°C indicating the combustion reactions had been quenched by cooling and dilution with ambient air and (ii) an infrared camera was used to continuously monitor the location of the plume and hood adjustments were made accordingly. The plume gases were sampled from the exhaust duct (see **Fig. 1**) and sent to gas analyzers to measure the mole fraction of the species important for determining combustion and destruction efficiencies. **Table 1** provides the make and model information, the instrument accuracy and the calibrated ranges of species mole fractions for the gas analyzers used in the study. A multi-gas analyzer was used to measure CO_2 and CO based on single-beam single-wavelength infrared absorption spectroscopy at a sample rate of one second. Gas chromatography (GC) with a flame ionization detector was used to measure CH_4, C_2H_4, C_2H_6, and C_3H_8 at discrete five-to-seven-minute intervals. Prior to starting experiments, ambient measurements of each species were recorded for background correction.

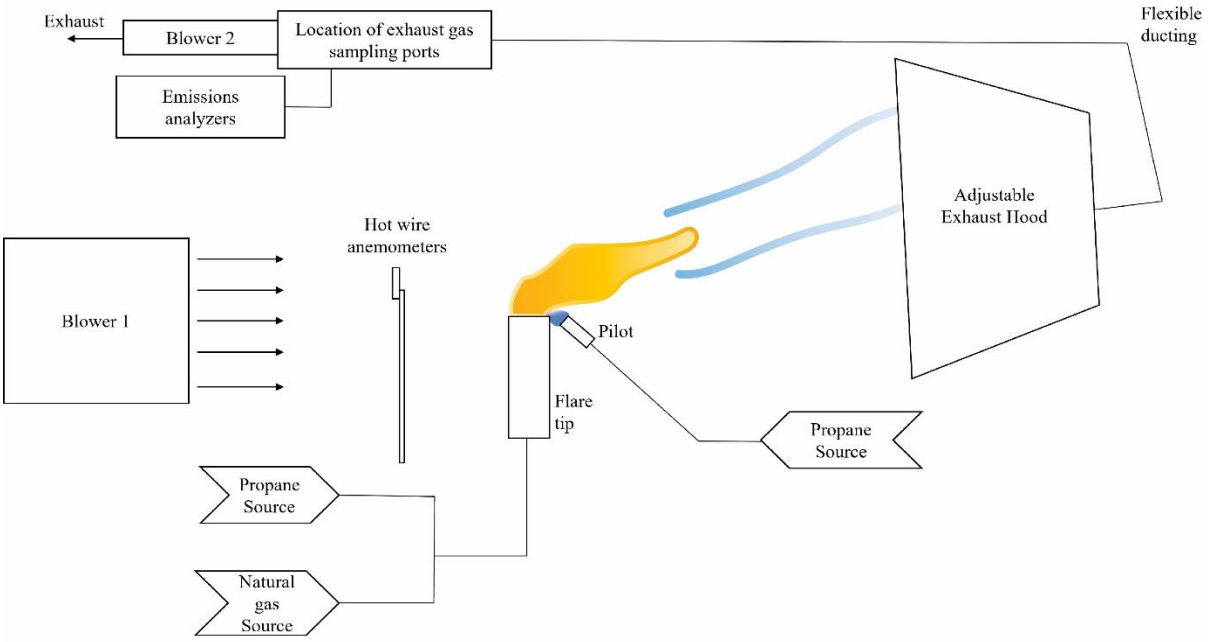

Fig. 1. Schematic of the experimental setup.

Either natural gas (NG) with a composition of 95.8% CH_4, 1.90% C_2H_6, 0.17% CO_2, 2.00% N_2, 0.08% C_3H_8 by volume (balance C_4 and higher hydrocarbons) or a blend of 80% propane and 20% NG by volume was used as the flare gas. A 3-inch schedule-40 pipe was used as the flare tip geometry, and a pilot ignition source fueled with propane was continuously lit throughout the experiments. The pipe flare was tested over a range of flow rates, gas compositions, and blower frequencies (i.e., crosswind speeds). The details of the test matrix are provided in **Table 2**.

Table 1. Emissions analyzers specifications.

Measurement system	**Sample frequency [Hz]**	**Principle of detection**	**Species**	**Range**	**Accuracy**
Servopro MultiExact 4100	1.0	Single beam single wavelength infrared	CO_2	0.0 – 10.0 %vol*	<1% full-scale
			CO	0.0 – 1.0 %vol*	<1% full-scale
Gas chromatography	0.002 - 0.003	Flame ionization detector	CH_4	0 – 100 ppm**	± 0.5 ppm
			C_2H_4	0 – 50 ppm**	
			C_4H_6		
			C_3H_8		

*Based on manufacturer specifications
**Based on calibration

Table 2. Experimental conditions tested.

Gas composition	**LHV [BTU/scf]***	**Flow rate [MSCFD]****	**Blower frequency [Hz]**
100% natural gas	910	5.0	0, 40
		10.0	60
		25.0, 50.0	40, 50, 60
80% propane / 20% NG (80/20 blend)	1,970	5.0	0, 40, 50
		25.0	30, 50, 60

*BTU/scf = British thermal units per standard cubic feet
**MSCFD = 1000 standard cubic feet per day

ii. Methodology for determining combustion and methane destruction efficiencies

For gas flaring, combustion efficiency (CE) is defined as the ratio between carbon in the form of CO_2 and total carbon in the flare plume [5]:

$$CE = \frac{X_{CO_2,plume} - X_{CO_2,\infty}}{(X_{CO_2,plume} - X_{CO_2,\infty}) + (X_{CO,plume} - X_{CO,\infty}) + \sum \#_{C,C_mH_n}(X_{C_mH_n,plume} - X_{C_mH_n,\infty})} \quad (1)$$

where X_{CO}, X_{CmHn}, and X_{CO2} are the gaseous mole fractions of each species and the subscripts define the locations as in the plume ('plume') or background ambient air ('∞'), and #C is the carbon number of each hydrocarbon (e.g., two for ethane or three for propane, etc.).

The equation for methane destruction removal efficiency was adapted from McDaniel [5] and is given by

$$DRE_{CH4} = 1 - \left[\frac{\frac{X_{CH_4,plume} - X_{CH_4,\infty}}{(X_{CO_2,plume} - X_{CO_2,\infty}) + (X_{CO,plume} - X_{CO,\infty}) + \sum \#_{C,C_mH_n}(X_{C_mH_n,plume} - X_{C_mH_n,\infty})}}{\frac{X_{CH_4,FG}}{X_{CO_2,FG} + X_{CO,FG} + \sum \#_{C,C_mH_n} X_{C_mH_n,FG}}} \right] \quad (2)$$

Like CE, it is only a function of mole fractions of the measured products in the plume gas. Both CE and DRE_{CH4} calculations take into account ambient (background) mole fractions of the various species.

A propagated uncertainty analysis was completed for CE and DRE_{CH4} which considers each species measurement as an independent source of error, given by

$$u_{CE} = \sqrt{\sum_{i=1}^{n} \left(\frac{\partial CE}{\partial j_i}\right)^2 u_{j_i}^2} \quad (3)$$

and

$$u_{DRE_{CH4}} = \sqrt{\sum_{i=1}^{n} \left(\frac{\partial DRE_{CH4}}{\partial j_i}\right)^2 u_{j_i}^2} \quad (4)$$

where *j* denotes the species (i.e., CO_2, CO, C_mH_n, etc.) in Eqs. 1 and 2. The uncertainty associated with the inlet methane concentration for DRE_{CH4} is assumed to be negligible.

The species measurements in the current study used different data acquisition rates (see **Table 1**). The following procedure was used to reconcile the data and determine combustion and methane destruction efficiencies of the flare. The measured CO_2 and CO emissions were averaged over a one-minute interval centered on the sampling time of the GC measurement. The primary source of error for the CO and CO_2 measurements were due to fluctuations in the crosswind and ambient environment that affected downstream measurements. The errors in CO and CO_2 were quantified by calculating the standard deviation of the one-minute interval centered at the time of the GC measurement. The hydrocarbon species (i.e., CH_4, C_2H_4, C_2H_6, and C_3H_8) were measured at discrete times for each test condition. These discrete measurements were used to calculate the combustion and methane destruction efficiencies. Additionally, the average of each species was calculated over the entire test interval, with the standard deviation representing the measurement uncertainty. The average combustion and methane destruction efficiencies were then calculated for each test condition.

III. Experimental Results

Fig. 2 shows instantaneous images of the 80/20 blend flare subjected to increasing crosswind. All images are for a flare gas flow rate of 25.0 MSCFD. As seen in the images, the flame was highly luminous at the lower crosswind condition (**Fig. 2a**) and the flames were nearly horizontal for all crosswind conditions. At higher crosswind speeds, the visible luminosity of the flame decreased due to the effects of increased air dilution. Notably, the flames were extremely turbulent and exhibited transient behavior due to the turbulent nature of the flames and due to fluctuations of the crosswind generated by the blower. The conditions presented in the images yielded decreasing CE as a function of increasing crosswind (from an average CE of 95.7% at the lowest crosswind condition to 87.6% at the highest crosswind condition). Natural gas exhibited similar trends as observed with the 80/20 blend; however, the flame was less luminous.

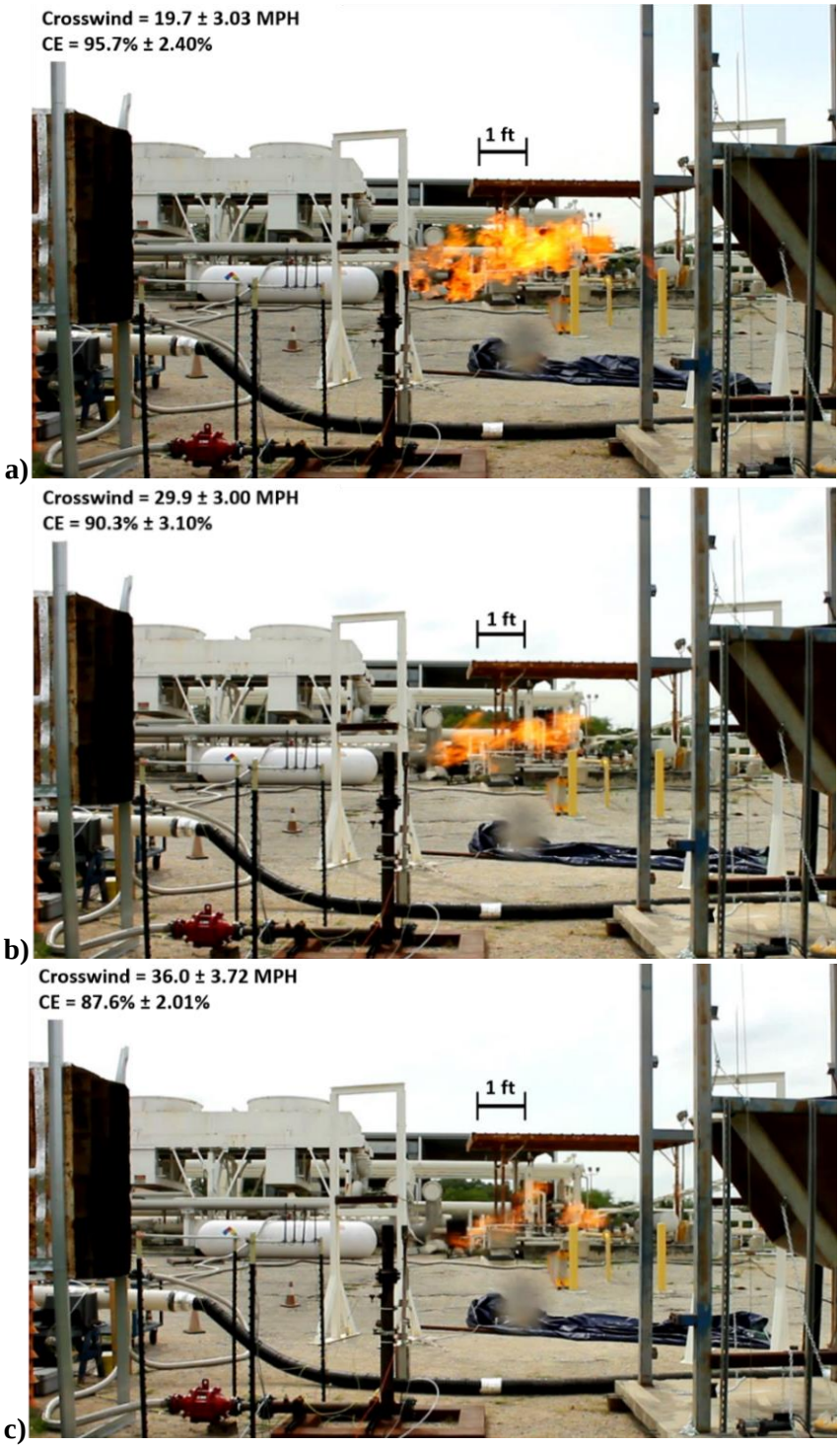

Fig. 2. Instantaneous images of 80/20 blend flames with flare gas flow rate of 25.0 MSCFD subjected to increasing crosswind from the top image to the bottom image with blower frequency of: a) 30 Hz, b) 50 Hz, and c) 60 Hz. Corresponding average crosswind speed, combustion efficiency, and uncertainty are provided in the images. Image contrast has been increased for clarity.

Time-dependent CO, CO_2, and crosswind speed measurements are shown in **Fig. 3** for natural gas and the 80/20 propane/NG blend, and the dashed lines represent the time when the GC samples were acquired (i.e., the CH_4, C_2H_4, C_2H_6, and C_3H_8 measurements were made) The zero-minute mark corresponds to the

time at which the test conditions were initially set, i.e., when the blower fan frequency and flare-gas flow rate were set to target values. The emission data typically stabilized after three to five minutes for the first test condition (from start-up at ambient temperature), with subsequent transitions taking about one to two minutes to stabilize. **Fig. 3** shows measurements from operating conditions after the first test conditions.

The crosswind speed was measured adjacent to and upstream of the flare tip. The average crosswind speed for the 50 Hz blower condition (**Fig. 3a** and **Fig. 3b**) was approximately 30 MPH and about 36 MPH for the 60 Hz condition (**Fig. 3c** and **Fig. 3d)**. All conditions in **Fig. 3** experienced turbulent fluctuations from the blower as indicated by the variability in crosswind speed over the test period.

For both natural gas and the 80/20 blend, there is a general decrease in background corrected CO_2 emissions as a function of crosswind speed from approximately 400 ppm to 300 ppm for NG (**Fig. 3a and Fig. 3c**) and 1400 ppm to 1000 ppm for the 80/20 blend (**Fig. 3b and Fig. 3d)**. CO emissions for all conditions in **Fig. 3** were below approximately 20 ppm. Most notably, the CO_2 emissions data show some variability as a function of time for all conditions. The results indicate dynamic effects from the turbulent flame and fluctuations created by the crosswind blower play an important role when assessing flare performance.

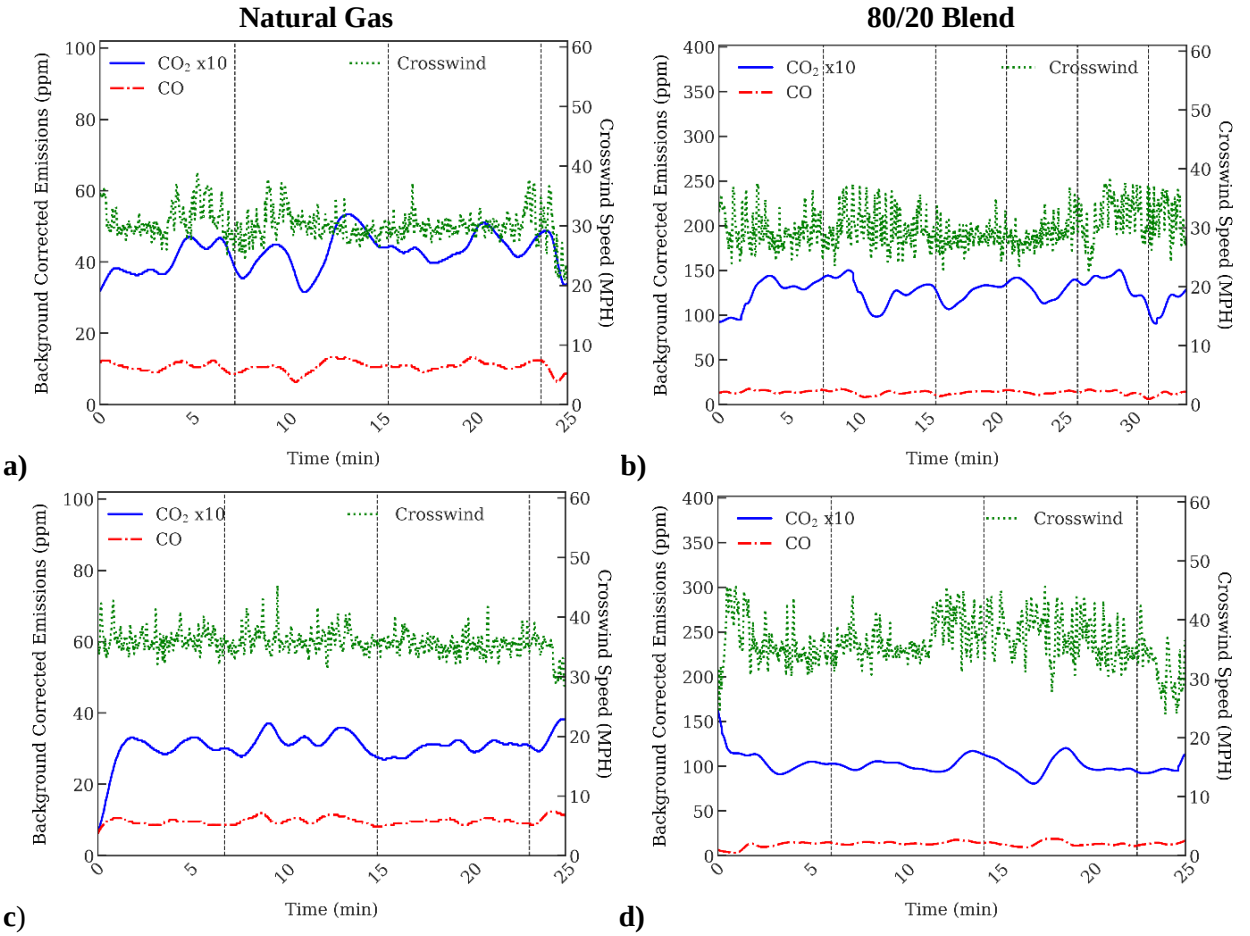

Fig. 3. Effects of crosswind speed on CO and CO_2 emissions and crosswind speed at a blower frequency of 50 Hz for a) NG (average crosswind speed of 30.2 ± 1.96 MPH) b) 80/20 propane/NG (average crosswind speed of 29.9 ± 3.00 MPH); and at a blower frequency of 60 Hz for c) NG (average crosswind speed of 35.7 ± 3.46 MPH) and d) 80/20 propane/NG blend (average crosswind speed of 36.0 ± 3.72 MPH). All data are for a flare gas flow rate of 25.0 MSCFD. The time when GC samples were acquired are shown as the black dashed vertical lines. Note the CO and CO_2 measurements are background corrected. The crosswind data presented were measured upstream of the flare tip.

Fig. 4 presents the background corrected species emissions data and corresponding combustion efficiencies for the test results in **Fig. 3** and for lower crosswind speeds. The CO and CO_2 data were averaged over one-minute intervals centered at the GC sample time shown in **Fig. 3**, and the error bars for CO and CO_2 represent one standard deviation from the mean. The error bars for the hydrocarbons are the uncertainties in the GC measurements (see **Table 1**). The error bars for the combustion efficiency are the propagated uncertainties associated with the species measurements.

The effect of crosswind on the natural gas results (**Fig. 4a**) is characterized by a general decrease in CO_2 as the crosswind speed increased from 24.5 to 35.7 MPH. Methane (as opposed to ethane, ethylene, or propane) was the primary hydrocarbon observed in the plume for conditions with lower CE and DRE_{CH4} values. The maximum methane emissions measured was 81 ppm for the highest crosswind speed, and no other hydrocarbons were detected for the conditions presented in **Fig. 4a**. While the absolute value of methane does not strictly increase as a function of increasing crosswind speed, the *relative* amounts of the species translate to lower combustion efficiencies at higher crosswind speeds. Carbon monoxide emissions remained relatively constant throughout each test, and below approximately 20 ppm. The emissions fluctuations shown in **Fig. 3** propagate to combustion efficiency measurements. For example, for NG flow rate of 25.0 MSCFD and an average crosswind speed of 30.2 MPH with yielded CE between 83.8% and 93.3%. The range for CE decreased to 76.6% to 80.7% for NG flow rate of 25.0 MSCFD and 35.7 MPH average crosswind speed.

The 80/20 blend experiments (**Fig. 4b**) showed some similar trends as observed with the NG tests. CO_2 generally decreased as crosswind increased; however, CO_2 was generally higher and unburned hydrocarbons were generally lower than observed with the NG experiments, translating to overall higher combustion efficiency. The primary unburned hydrocarbon measured was propane, and the recorded value was 47 ppm. Other hydrocarbons (shown in **Fig. 4b**) were below approximately 10 ppm. The 80/20 blend yielded higher CE compared with NG, with CE values between 91.0% and 92.3% for 29.9 MPH crosswind speed and 85.5% to 91.8% for the 36.0 MPH crosswind speed condition. The findings of relatively high CE for flares with higher heating value gases are consistent with prior research on flares in crosswind [13-16].

The average species emissions from **Fig. 3** and **Fig. 4** were combined to calculate the average combustion and methane destruction efficiencies, and are presented in **Fig. 5** and **Fig. 6** as a function of average crosswind speed for the natural gas and 80/20 blend experiments and the different flare gas flow rates. The vertical error bars are the propagated uncertainties due to the uncertainties in the species measurements and the horizontal error bars are one standard deviation based on the average crosswind speed. The results show the strong correlation between CE and DRE_{CH4}, with DRE_{CH4} generally measuring higher than CE. The results also show the uncertainty in CE and DRE_{CH4} is up to ±4.5%, and is primarily due to the variability in species measurements at the same test conditions. The NG results (**Fig. 5a** and **Fig. 6a**) show CE decreased as crosswind increased, with lower flow conditions (≤ 10 MSCFD) showing increased sensitivity to crosswind speed. Higher flow conditions (≥ 25 MSCFD) showed more resistance to crosswind effects indicated by higher CE. The 80/20 blend (**Fig. 5b** and **Fig. 6b**) showed similar trends as NG between similar flow-rate conditions. However, the blend yielded higher CE when compared with NG at the same flow rate and crosswind conditions. This finding is also consistent with previous wind tunnel studies [13-16] where, in general, higher combustion and destruction efficiencies were observed with higher flare gas flow rates and higher heating value fuels.

It should be noted that the 80/20 blend flames were visibly sooting for all flare gas flow rates with crosswind speeds below approximately 5 MPH, similar to findings by Stolzman et al. [18], where pure propane was used as the flare gas. Soot was not directly measured in the current work, and there is limited and somewhat conflicting data in the literature regarding the contribution of soot to combustion efficiency measurements. Pohl et al. [19] found soot from smoking flares to account for less than 0.5% of measured combustion inefficiencies; however, the study showed data from a single condition where the flare gas composition was 56% propane in nitrogen which has a significantly lower heating value than the 80/20 blend used in the current work. McDaniel [5] evaluated the effect of soot on CE of visibly smoking flares using crude propylene as the flare gas. McDaniel estimated that CE was over-reported between 1.62% for

'lightly' smoking flares and up to 8.59% for 'heavily' smoking flares. For minimal or non-smoking flares (e.g., the natural gas in the current work), soot had a negligible effect on CE. Sooting likely affects CE under some conditions; however, there is no standard practice for how to effectively measure and incorporate soot emissions into CE determinations. Thus, the results presented in **Fig. 5b** and **Fig. 6b** only consider gas-phase species, and soot is not accounted for in the calculations.

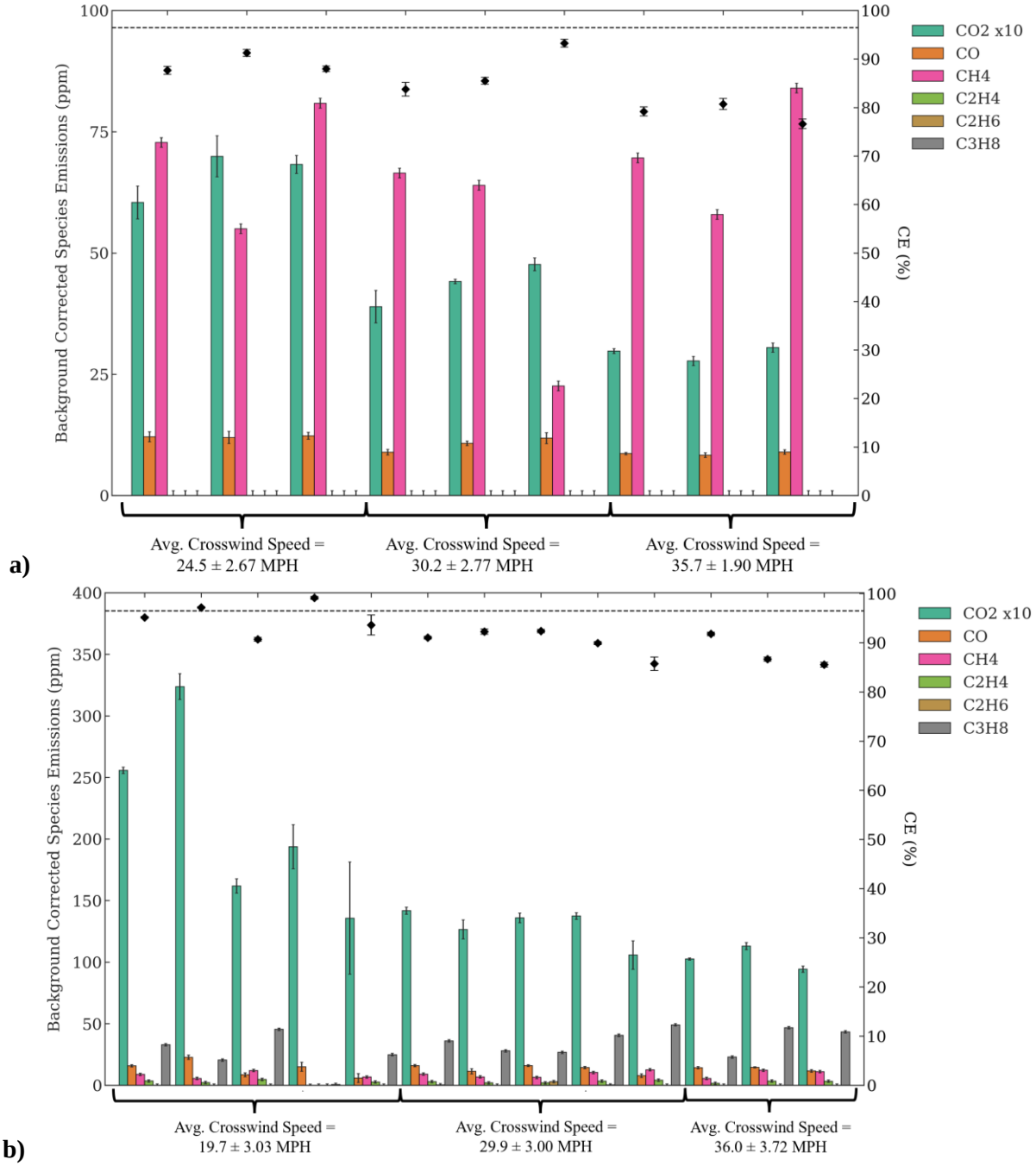

Fig. 4. Background corrected species emissions and associated combustion efficiencies for flare gas flow rate of 25.0 MSCFD for (a) NG and (b) 80/20 propane/NG blend. The black dashed horizontal line is the minimum combustion efficiency of 96.5% assumed for US EPA compliant field-scale flares. Error bars represent the uncertainty of the species data (including the uncertainty of the background measurements) and the propagated uncertainty for the CE results.

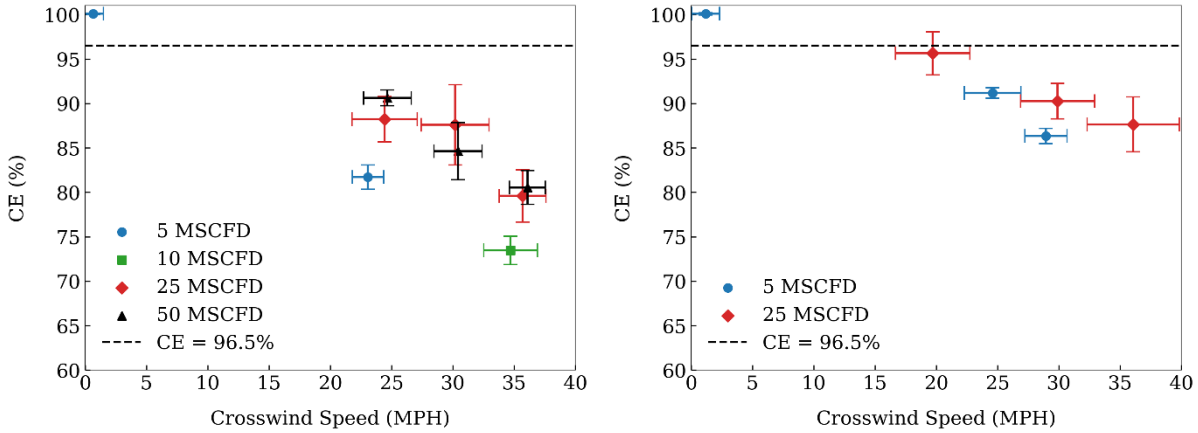

Fig. 5. Effects of crosswind speed and flare gas flow rate on combustion efficiency for (a) natural gas experiments and (b) 80/20 blend experiments (uncorrected for soot). The black dashed line is the minimum combustion efficiency of 96.5% assumed for US EPA compliant field-scale flares. The vertical error bars are the propagated uncertainty due to the uncertainty of the species measurements used to calculate CE. The horizontal error bars are one standard deviation from the average crosswind speed. Note the highest efficiencies have uncertainties smaller than the symbol size.

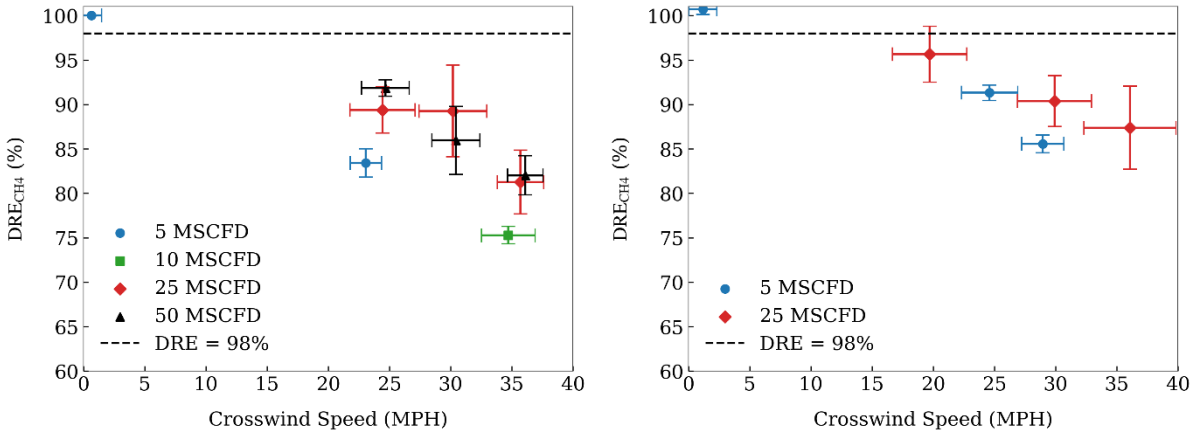

Fig. 6. Effects of crosswind speed and flare gas flow rate on methane destruction removal efficiency for (a) natural gas experiments and (b) 80/20 blend experiments (uncorrected for soot). The black dashed line is the minimum destruction efficiency of 98% assumed for US EPA compliant field-scale flares. The vertical error bars are the propagated uncertainty due to the uncertainty of the species measurements used to calculate DRE_{CH4}. The horizontal error bars are one standard deviation from the average crosswind speed. Note the highest efficiencies have uncertainties smaller than the symbol size.

IV. Comparison with prior work

Several studies [13-16] have developed scaling relationships for non-assisted pipe flares to try and understand trends for different crosswind conditions. Past studies have found combustion efficiency of a flare, using a constant fuel source such as natural gas or propane, is a function of the crosswind velocity, flare gas exit velocity, and the pipe diameter. The semi-empirical relationships developed by Johnson and Kostiuk [13], Howell [14], and Burtt [16] are based on the Richardson number (refer to Johnson and Kostiuk for additional information regarding the development of the scaling parameter [13, 20]), and all follow the same general relationship:

$$1 - CE \propto \frac{U_\infty}{(gDV_j)^{\frac{1}{3}}} \quad (5)$$

where 1 – CE is the combustion inefficiency, U_∞ is the crosswind velocity, g is gravity, D is the outer pipe diameter, and V_j is the flare gas exit velocity. The scaling parameter represents the relative strength of the crosswind speed to the speed of the jet, and other forms of this equation designate a similar term [15].

Burtt [16] and Burtt et al. [21] conducted flare experiments in a closed-loop wind tunnel capable of generating up to 10 m/s (22 MPH) crosswind. The facility featured four fans placed approximately 15-20 meters downwind of the flare, and a passive turbulence grid was used to generate turbulence in the incoming crosswind to the flare. The study investigated 1", 2", 3" and 4" pipe flares, where 3" and 4" flares are commonly found at upstream oil and gas production sites in Canada [22,23]. Crosswind measurements were taken using a pitot tube located downstream of the flare. Plume emissions (CO_2, CO, CH_4, C_2H_6, and N_2O) were measured downstream of the flare using various gas analyzers. The method for calculating combustion efficiency accounted for accumulation rates of species emissions within the wind tunnel [21].

Data from Burtt [16] and Stolzman et al. [18] were compared with results from the current work due to the similar test conditions and pipe diameter. **Table 3** summarizes the conditions and **Table 4** provides the gas compositions of the prior studies and the current work. Only data from tests using flare gas compositions comparable to natural gas were used for the comparisons presented here.

Table 3. Flare conditions of previous and current studies of utility flares.

	Burtt [16]	**Stolzman et al. [18]**	**Current work**
Pipe diameter (in)	1, 2, 3, 4	3	3
Flare exit velocity (m/s)	0.5, 1, 2	0.5, 3.4	0.3, 0.7, 1.7, 3.4
Crosswind (m/s)	1.5 – 11.5	0 – 5.9	0 – 16.1
Flare gas composition	• M6* • L6*	• Natural gas*	• Natural gas*
LHV (BTU/scf)	• M6: 1,009 • L6: 865	910	910

***See Table 4**

Table 4. Flare gas compositions used in the studies listed in Table 3

	CH_4 (%vol)	**C_2H_6 (%vol)**	**C_3H_8 (%vol)**	**C_4H_{10} (%vol)**	**N_2 (%vol)**	**CO_2 (%vol)**
M6 [16]	86.03	6.81	2.35	1.99	1.61	1.21
L6 [16]	93.31	0.32	0.09	0.27	1.38	4.64
Natural gas (NG)*	95.70	1.90	0.10	0.03	2.00	0.20

*Natural gas used in Stolzman et al. [18] and the current work

Fig. 7 shows the combustion inefficiency as a function of crosswind, including data from Burtt [16], Stolzman et al. [18] and the current work for 3" pipe flares. All data were acquired at similar flare-gas flow rates and using similar flare-gas compositions. The results show consistent trends, where the combustion inefficiency increases non-linearly with increasing crosswind for all studies. There is good quantitative agreement in the combustion inefficiency at conditions with no cross-flow. While no error bars are provided for the data from Burtt [16], their wind tunnel results are consistently lower than the results from Stolzman et al. [18] and the current study at conditions with non-zero crosswind. The discrepancy may be due to dissimilarities in the turbulent structures of the crosswind created in the wind tunnel studies compared with the blower used in Stolzman et al. [18] and the current work. Another key distinction between the studies is the use of a pilot flame with the flare. The current work and the study by Stolzman et al. [18] both used

pilot flames as required by US regulations and the wind tunnel studies by Burtt [16] did not. However, a pilot flame is expected to provide greater flame stability, which would be expected to increase combustion efficiency. The results presented in **Fig. 7** indicate the pilot flame has less effect than the characteristics of the crosswind.

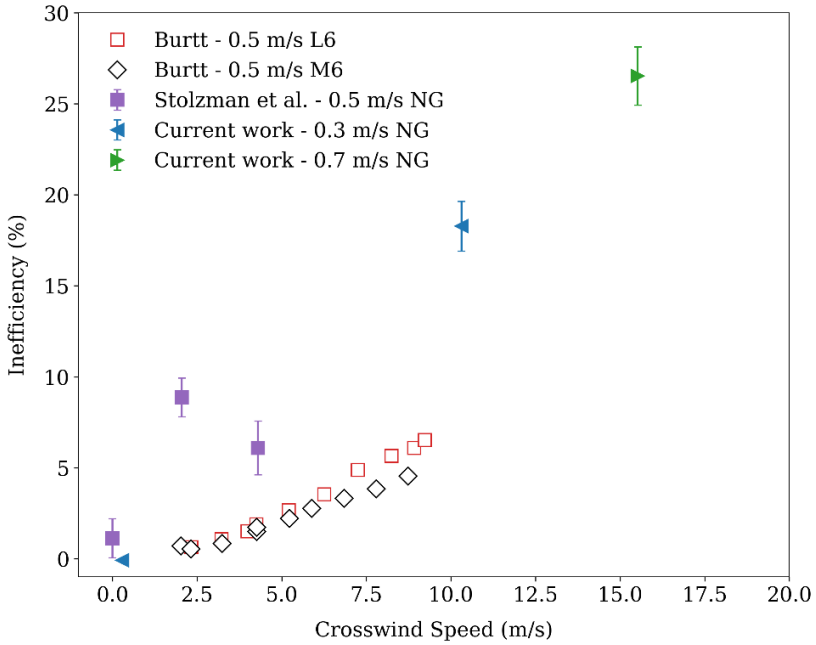

Fig. 7. Comparison of combustion inefficiency for 3" pipe flares. Data from Burtt [16] and Stolzman et al. [18] shown for 3" pipe flare tests only.

The effectiveness of the scaling correlation (**Eq. 5**) on capturing effects of crosswind speed and flare pipe diameter for the results of the current and prior work is presented in **Fig. 8**. Again, the general trends are consistent between the different data sets, where combustion inefficiency appears to scale exponentially with the dimensionless ratio of gas speeds. However, the absolute values and scatter in the data sets differ, which again may be due to differences in the turbulence characteristics. The differences suggest a critical aspect of the turbulence is not being captured in the scaling parameter based on average flare gas and wind speeds. Further investigation into turbulent effects and their integration into a scaling parameter may provide a more accurate scaling of flare performance under varying crosswind conditions.

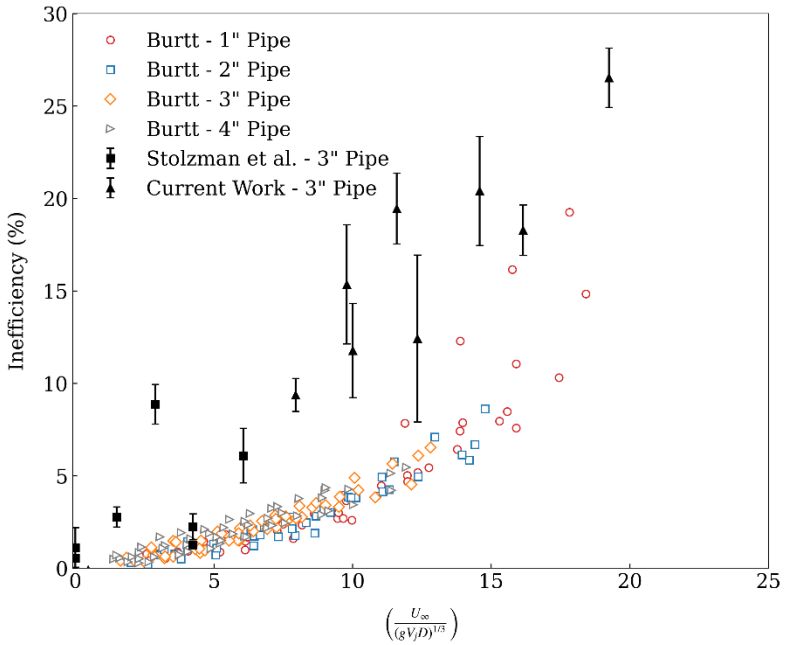

Fig. 8. Combustion inefficiency as a function of the dimensionless scaling parameter (Eq. 5) for data from Burtt [16], Stolzman et al. [18], and the current work.

V. Conclusions

The current work demonstrated a new method for evaluating the combustion and methane destruction efficiencies of non-assisted flares over a range of conditions important to low-flow flaring at industrially-relevant conditions (flare gas flow rates of 5.0 to 50.0 MSCFD). A new outdoor flare facility was developed that included a large moveable outdoor hood with extractive sampling and a blower capable of generating crosswinds of up to 40 MPH. Time-resolved emissions measurements captured fluctuations in the crosswind and species measurements that translated to fluctuations in the associated combustion and methane destruction efficiencies. Low-flow (≤10 MSCFD) natural gas flares under crosswind conditions exhibited lower average combustion efficiencies compared with higher flow rate conditions (≥25 MSCFD) (77.6% compared with 85.2%). The 80/20 propane/natural gas blend showed higher average combustion efficiencies compared with natural gas when subjected to crosswind (90.2% compared with 83.3%); but combustion efficiencies remained below 95% with these higher BTU flare gases for crosswind speeds greater than approximately 20 MPH and flare gas flow rates of 5.0 and 25.0 MSCFD. Comparisons between the current and previous work showed consistent trends, but some differences in absolute values for combustion inefficiency. A scaling law based on the ratio of windspeed to a weighted average flare gas speed captured some of the trends in the current and prior work, but the experimental data exhibit some systematic differences and scatter, which may be an indication of the effects of complex turbulent interactions. In addition to important new experimental data, the experimental protocols and methods demonstrated in this work provide a valuable new framework for flare performance studies.

Acknowledgements

The information, data, or work presented herein was funded in part by the Advanced Research Projects Agency-Energy (ARPA-E), U.S. Department of Energy, under Award Number DE-AR0001534. The views and opinions of authors expressed herein do not necessarily state or reflect those of the United States Government or any agency thereof.

References

[1] US Environmental Protection Agency, Compilation of Air Pollutant Emissions Factors from Stationary Sources (AP-42), Volume I, (2024), available at < https://www.epa.gov/air-emissions-factors-and-quantification/ap-42-compilation-air-emissions-factors-stationary-sources >.

[2] US Government Publishing Office, CFR-2016-title40-vol12-sec63-670, Requirements for flare control devices. available at <https://www.govinfo.gov/content/pkg/CFR-2016-title40-vol12/pdf/CFR-2016-title40-vol12-sec63-670.pdf>, downloaded July 8, 2024.

[3] G. Plant, E.A. Kort, A.R. Brandt, Y. Chen, G. Fordice, A.M. Gorchov Negron, S. Schwietzke, M. Smith, D. Zavala-Araiza, Inefficient and unlit natural gas flares both emit large quantities of methane, Science 377 (2022) 1566-1571.

[4] J.L. Sorrels, J. Coburn, K. Bradley, D. Randall Section 3 VOC Destruction Controls. Chapter 1. Flares US Environmental Protection Agency (2019) available at https://www.epa.gov/sites/default/files/2019-08/documents/flarescostmanualchapter7thedition_august2019vff.pdf

[5] M. McDaniel, Flare efficiency study, US EPA Report: EPA-600/2-83-052, Industrial Environmental Research Laboratory (1983).

[6] J.H. Pohl, N. Soelberg, Evaluation of the Efficiency of Industrial Flares: Flare Head Design and Gas Composition, US EPA Report: EPA- 600 /2-85-106, Air and Energy Engineering Research Laboratory (1985).

[7] J.H. Pohl, R. Payne, J. Lee, Evaluation of the Efficiency of Industrial Flares: Test Results, US EPA Report: EPA- 600 /2-84-095, Energy and Environmental Research Corporation (1984).

[8] Marathon Petroleum Company, Performance Test of a Steam-Assisted Elevated Flare with Passive FTIR. Texas City (2010).

[9] Marathon Petroleum Company, Performance Test of a Steam-Assisted Elevated Flare with Passive FTIR – Detroit (2010).

[10] D.T. Allen, V.M. Torres, TCEQ 2010 Flare Study Project Final Report, The University of Texas at Austin, The Center for Energy and Environmental Resources (2011).

[11] US Environmental Protection Agency, Parameters for Properly Designed and Operated Flares, US EPA Office of Air Quality Planning and Standards (OAQPS) (2012).

[12] US Department of Energy, Office of Oil and Natural Gas, Office of Fossil Energy, Natural Gas Flaring and Venting: State and Federal Regulatory Overview, Trends, and Impacts, (2019) available at <https://www.energy.gov/fecm/articles/natural-gas-flaring-and-venting-regulations-report>.

[13] M.R. Johnson, L.W. Kostiuk, A parametric model for the efficiency of a flare in crosswind, Proc. Combust. Inst. 29 (2) (2002) 1943-1950.

[14] L. Howell, Flare Stack Diameter Scaling and Wind Tunnel Ceiling and Floor Effects on Model Flares, M.Sc. thesis, University of Alberta, Canada, 2005.

[15] P. Gogolek, Explaining the “three inch rule”: Why model flares don’t match full-scale, American Flame Research Committee (AFRC) Indust. Combust. Symp. (2022) 1-18.

[16] D. Burtt, Efficiency and Emission Rates of Flares in a Turbulent Crosswind, M.Sc. thesis, Carleton University, Canada, 2022.

[17] J. Stolzman, A. Mohit, L. Gutierrez, J. Capecelatro, M.S. Wooldridge, New challenges in waste gas flaring in upstream oil and gas, International Gas Research Conference (IGRC) (2024) 1-11.

[18] J. Stolzman, L. Gutierrez, A. Schluneker, M.S. Wooldridge, An experimental study of the effects of waste-gas composition and cross-wind on non-assisted flares using a novel indoor testing approach, manuscript in preparation, 2024.

[19] J.H. Pohl, J. Lee, R. Payne, B.A. Tichenor, Combustion efficiency of flares, Combust. Sci. Tech. 50 (1986) 217-231.

[20] M.R. Johnson and L.W. Kostiuk, Efficiencies of low-momentum jet diffusion flames in crosswinds, Combustion and Flame. 123 (2000) 189-200

[21] D.C. Burtt, D.J. Corbin, J.R. Armitage, B.M. Crosland, A.M. Jefferson, G.A. Kopp, L.W. Kostiuk, M.R. Johnson, A methodology for quantifying combustion efficiencies and species emission rates of flares subjected to crosswind, Journal of the Energy Institute. 104 (2022) 124-132.

[22] J.D.N. McEwen and M.R. Johnson, Black carbon particulate matter emission factors for buoyancy-driven associated gas flows, J. Air Waste Manag. Assoc. 62(3) (2012) 307-321.

[23] B.M. Conrad and M.R. Johnson, Field measurements of black carbon yields from gas flaring, Environmental Science and Technology. 51(3) (2016) 1893-1900.